Deveaux et al., http://www.jcb.org/cgi/content/full/jcb.200808034/DC1

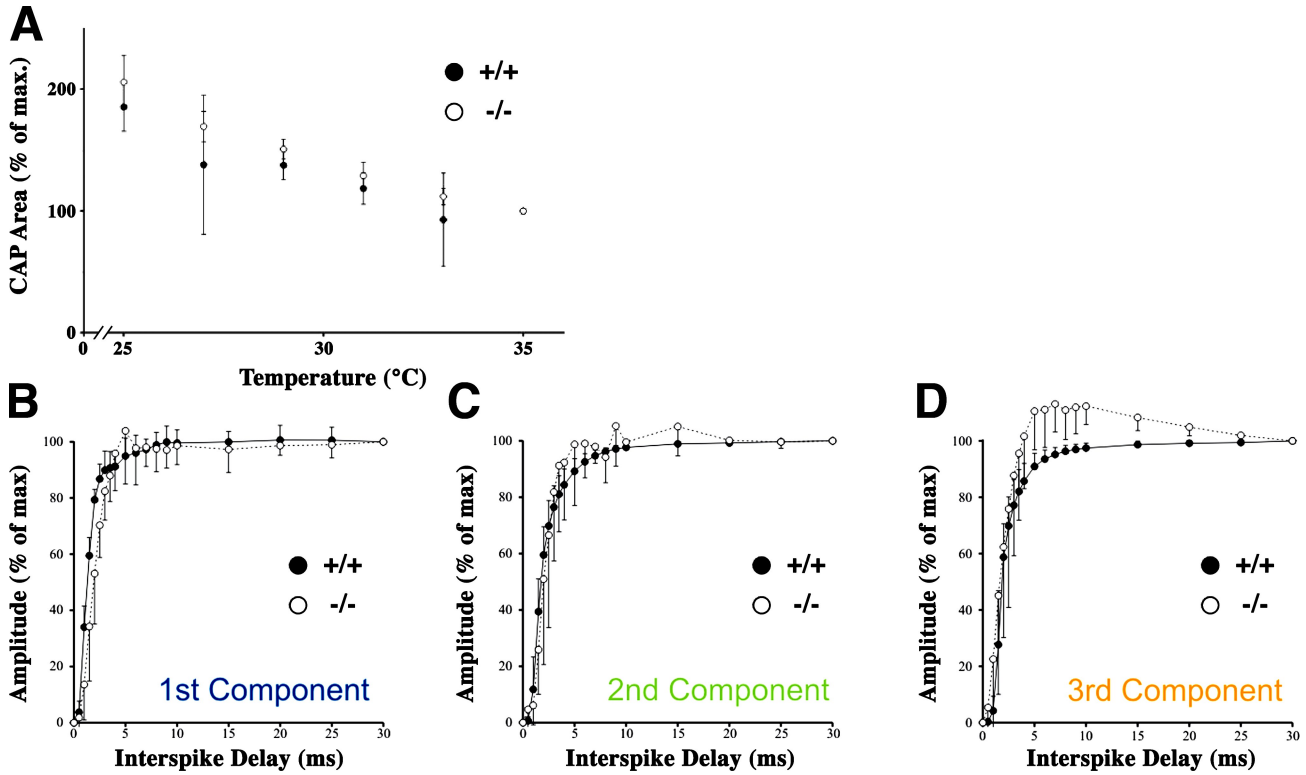

Figure S1. **Absence of conduction block in *Claudin 11*–null mice.** (A) Mean CAP area ($n = 6$) from wild-type (+/+) and *Claudin 11*–null mice (−/−) recorded as a function of temperature (35–25°C) and expressed as a percentage of the CAP area at 35°C. No differences between wild-type and mutant optic nerves are observed (two-tailed unpaired *t* test; $P < 0.05$). Lowering the bath temperature does not significantly improve CAP amplitudes or areas in mutant nerves, thereby ruling out any possibility that the diminished CAP amplitude is related to conduction block in the mutants. (B–D) The refractory period in *Claudin 11*–null optic nerves is normal, indicating that AP duration and repolarization are not affected by the absence of TJs. The supranormal period in the third component from *Claudin 11*–null mice corresponds temporally to the hyperpolarizing afterpotentials observed in Fig. 1 B. Error bars indicate SD.

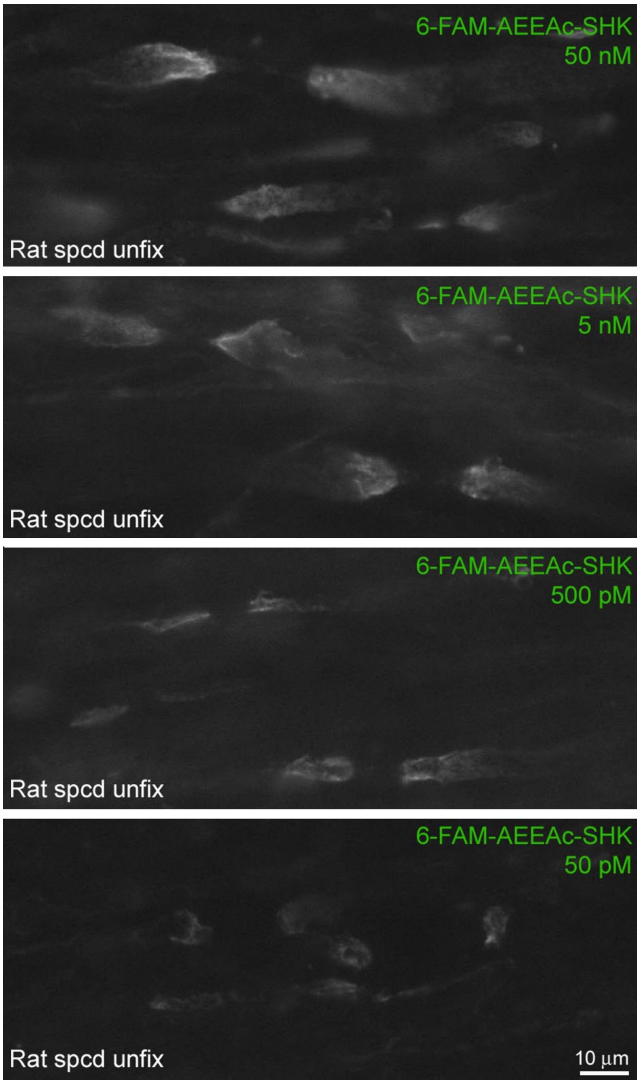

Figure S2. **Fluorescent peptide toxins bind to juxtaparanodal K^+ channels.** 10-µm cryostat sections of unfixed nonpermeabilized rat spinal cord are incubated in 50 pM–50 nM 6-FAM-SHK in PBS. At these concentrations, the toxin only labels juxtaparanodes and is optimal at 50 nM. Above 50 nM, some background staining is apparent. Nodes of Ranvier are not labeled. Spcd, spinal cord.

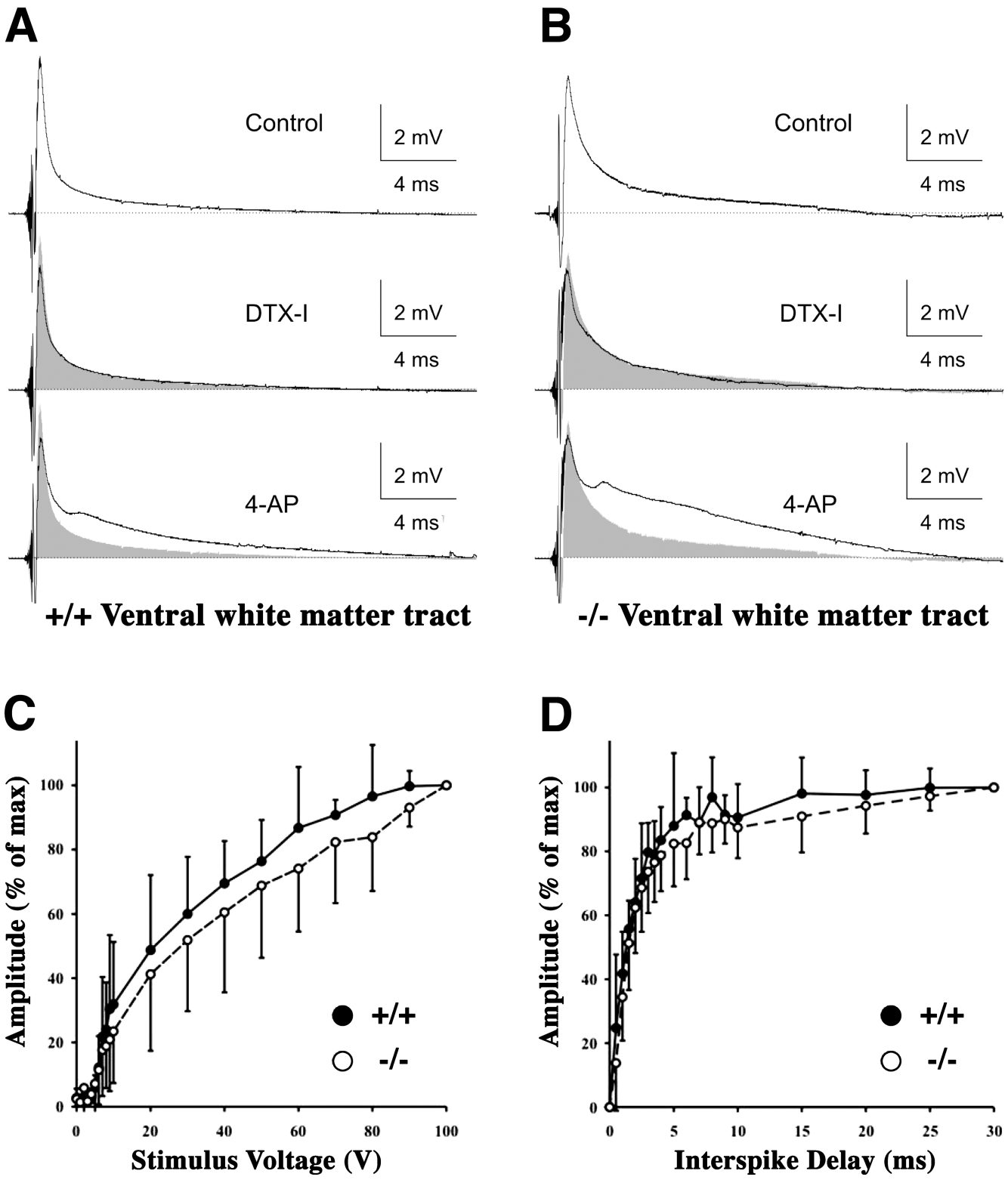

Figure S3. **Nerve conduction in spinal ventral column is moderately affected in *Claudin 11*–null mice.** (A and B) Recordings from spinal cord ventral columns in wild-type (A) and *Claudin 11–null* mice (B) treated with DTX and 4-AP as indicated. Although the CAP delays and amplitudes are similar for both genotypes, the duration of the CAPs is significantly longer in *Claudin 11*–null mice, which is indicative of conduction slowing in small axons. DTX has no effect on either wild-type or mutant animals. 4-AP broadens the CAPs from wild-type and null spinal cords similarly. No hyperpolarizing after-potentials are detected. Gray shading indicates CAPs from untreated spinal cords for comparison with drug treatments ($n = 7$; two-tailed nonpaired t test; $P < 0.05$). (C) Normal recruitment period in spinal cord ventral columns from *Claudin 11*–null mice. Recruitment of APs to the CAPs from wild-type (+/+) and *Claudin 11*–null mice (−/−) are not significantly different ($n = 7$; one-tailed nonpaired t test; $P < 0.05$). (D) Normal recruitment and refractory period in spinal cord ventral columns from *Claudin 11*–null mice. AP refractory period from wild-type (+/+) and *Claudin 11*–null mice (−/−) are not significantly different ($n = 7$; one-tailed nonpaired t test; $P < 0.05$). Error bars indicate SD.

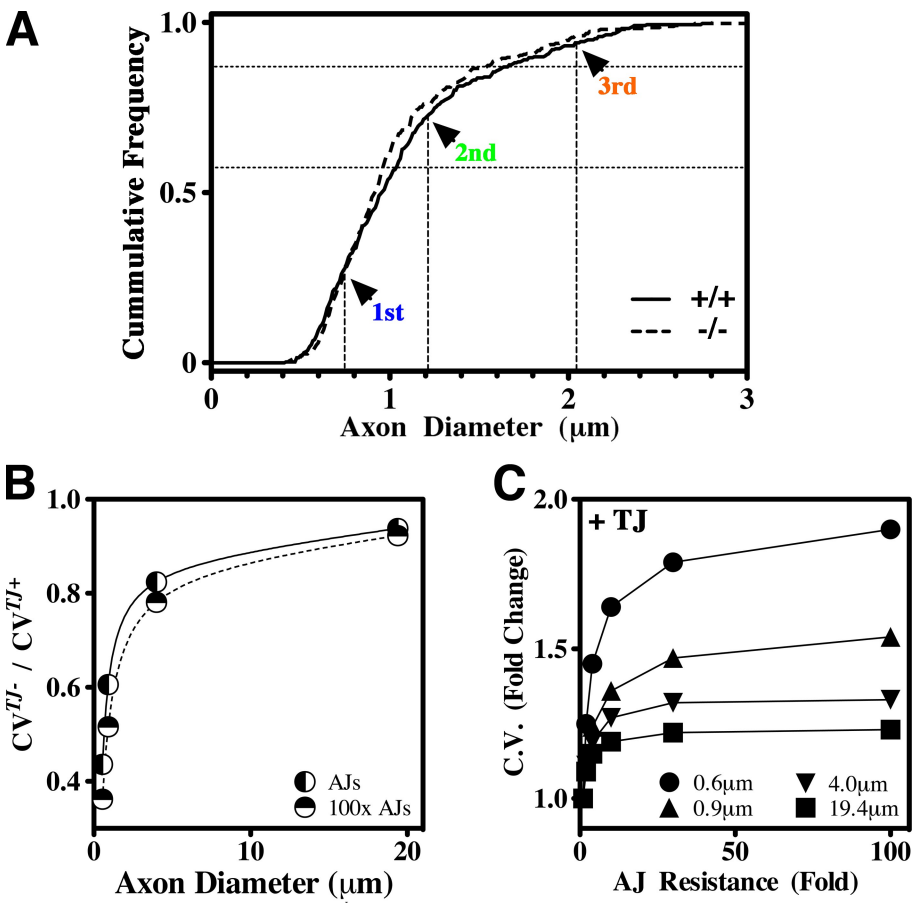

Figure S4. **Estimation of mean axon diameters corresponding to each CAP component in optic nerve.** TJs and axoglial junctions (AJ) serve different and independent functions in CNS myelinated axons. (A) To derive physiological data from the electrophysiological analysis of optic nerves in *Claudin 11*–null mice for comparison with the TJM and the DCM, we first determined the areas under the curve for each of the three components in the CAPs (Fig. 1, A and B). These areas approximate the proportions of the CAPs contributed by axons of different diameters in the optic nerves. Next, we generated cumulative frequency histograms from the optic nerve frequency histograms in Fig. 5 G and used the peak areas from the CAPs to calculate mean axon diameters for each component. (B) The ratio of CVs in the absence and presence of TJs is shown as a function of axon diameter. The solid curve is derived from Fig. 6 A (open circles) and represents TJM simulations using an axoglial junction resistance equivalent to twice that of the periaxonal space (i.e., based on 50% occupancy of the periaxonal space by the protein complexes forming the axoglial junctions). The dashed line represents TJM simulations when axoglial junction resistance is 100-fold higher than the periaxonal space (axoglial junctions are effectively electrically tight). These simulations demonstrate that the loss of TJs results in diminished CV independently of the electrical barrier properties of axoglial junctions, particularly in small axons. (C) The relative changes in CV from different fibers as a function of the resistance of axoglial junctions. These data are normalized to the CV for an axoglial junction that is equal to the resistance of the periaxonal space (i.e., no axoglial junctions). For axons of all diameters, CV increases significantly as axoglial junction resistance increases. These data are consistent with experimental data from axoglial junction mutant mice in which CV is reduced or blocked in all axons. These data reveal a major difference with TJs, which only significantly affect small fibers.

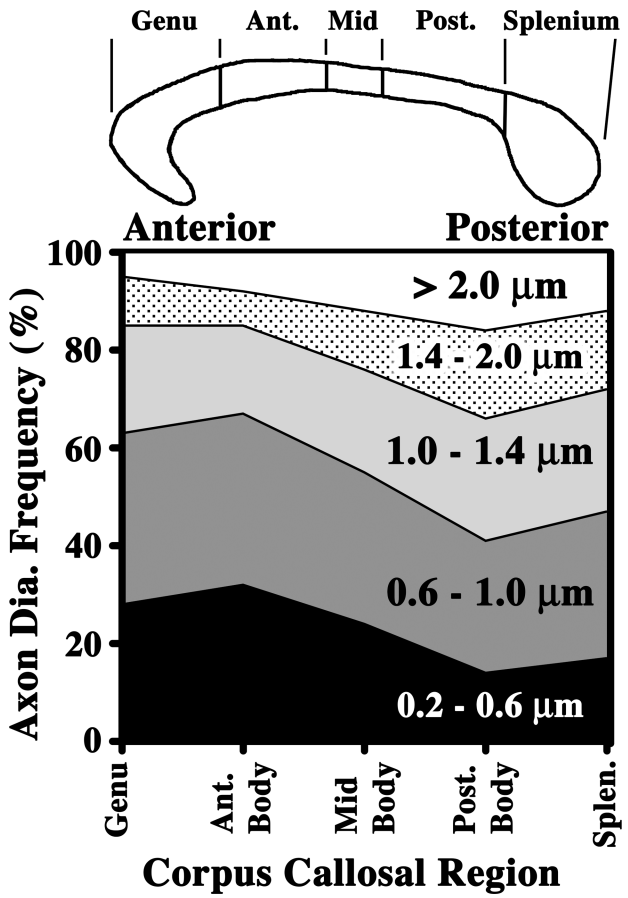

Figure S5. **Predominance of small myelinated axons in human corpus callosum.** Schematic of human corpus callosum in the sagittal plane showing division into five regions (Aboitiz, F., A.B. Scheibel, R.S. Fisher, and E. Zaidel. 1992. *Brain Res.* 598:143–153). In contemporary literature (Hofer, S., and J. Frahm. 2006. *Neuroimage.* 32:989–994), these regions approximately correspond to the Genu, which comprises fibers connecting prefrontal cortices of the left and right hemispheres; the anterior body (Ant.), which connects premotor and supplemental motor cortices; the midbody (Mid), which connects primary motor cortices; the posterior body (Post.), which connects primary sensory cortices; and Splenium, which connects higher order processing areas of the parietal and temporal lobes (anterior two thirds) and visual cortex (posterior one third). The graph details morphometry from electron micrographs of human corpus callosum adapted from Fig. 4 in Aboitiz et al. (Aboitiz, F., A.B. Scheibel, R.S. Fisher, and E. Zaidel. 1992. *Brain Res.* 598:143–153). The frequency distribution of small, medium, and large diameter axons is shown for each of the five regions of corpus callosum.

Table S1. **Morphometric analysis in optic nerves from wild-type and *Claudin 11*–null mice**

Parameter	*g* ratio		Axon diameter	
	+/+	−/−	+/+	−/−
			μm	μm
Minimum	0.75	0.62	0.42	0.44
25th percentile	0.81	0.8	0.73	0.75
Median	0.83	0.84	0.96	0.94
75th percentile	0.85	0.86	1.26	1.23
Maximum	0.91	0.94	2.81	3.31
n	328	325	328	325

Table S2. **Characteristics of CAPs recorded from spinal cord ventral columns of wild-type and *Claudin 11*–null mice**

Parameter	+/+	−/−
Amplitude V_{max} (mV)	2.95 ± 1.7	3.06 ± 1.29
Delay V_{max} (ms)	0.48 ± 0.06	0.55 ± 0.15
Delay $V_{1/2}$ (ms)	0.31 ± 0.05	0.35 ± 0.08
Duration $V_{1/2}$ (ms)	0.6 ± 0.06	1.02 ± 0.35[a]
Conduction velocity $V_{1/2}$ (ms^{-1})	23.3 ± 3.7	21.3 ± 5.2
Conduction velocity V_{max} (ms^{-1})	14.8 ± 1.8	13.5 ± 3.5
Conduction velocity V_{fall} (ms^{-1})	7.8 ± 0.8	5.6 ± 1.9[a]
Area	2,556 ± 1,054	3,817 ± 1,152
n	5	7

[a]Significantly different from controls (two-tailed nonpaired *t* test; $P < 0.05$).